Numerical Study on NO_x Production of Transitional Fuel Jet Diffusion Flame*

Hiroshi YAMASHITA**

A direct numerical simulation of a two-dimensional jet diffusion flame developed in a co-flowing air stream was carried out using the GRI [Gas Research Institute] chemical reaction mechanism (NO_x included) in order to elucidate the mechanism of NO_x formation in turbulent flow fields. The governing equations were discretized and numerically integrated using the finite volume method. The temperature dependence of thermodynamical properties was taken into account; transport properties were calculated according to the simplified transport model proposed by Smooke [Reduced Kinetic Mechanisms and Asymptotic Approximations for Methane-Air Flames, (1991), p. 1-28, Springer-Verlag]. Fuel jet velocity was found to have the same effects on the flame structure and the unsteady behavior as those concluded from the flame sheet approach; by increasing the fuel jet velocity, the flow becomes turbulent with large fluctuations downstream, and the flame is disturbed by the enlarged fluctuations in the turbulent region downstream where local extinction takes place. From a comparison with the laminar counterflow diffusion flame, it was concluded that the hypothesis of the laminar flamelet model that "the instantaneous local structure of the turbulent flow field can be accurately simulated by the laminar diffusion flame", can be applied to the unsteady turbulent jet flame that includes the possibility of extinction and takes into account the NO_x formation process. As a result, it was verified that the formation of NO_x in the turbulent flow field has the same mechanism as that in the unsteady laminar diffusion flame even for the case of extinction.

Key Words: Diffusion Combustion, Jet, Pollutant, Kinetics, Numerical Analysis, CH_4, Unsteady Behavior, NO_x

1. Introduction

Recently, the increase in the number of environmental problems has become the main concern all over the world. The conservation of energy and natural resources as well as the need to reduce atmospheric pollution has made the understanding of the combustion phenomenon an urgent issue. The turbulent diffusion flame is one of the most fundamental flames used in a wide variety of applications. Numerical simulation can be used to gain a better understanding of the turbulent mixing process and the structure of such flames to help in the development of highly efficient combustion systems and to realize an accurate estimation of hazardous emissions. The jet diffusion flame, with the most typical flow geometry, had been the subject of many numerical simulations carried out for turbulent diffusion flames[1]. The main concern was to elucidate the effects of heat release on flow characteristics and flame stability; such aspects were verified using simple methane-air kinetics such as the global non-reversible one-step mechanism[2]-[5] or the skeletal elementary reaction mechanism[6],[7]. Moreover, the correctness and the physical validity of the calculation method adopted have been verified by comparing with physical phenomena derived from experiments.

Based on such studies, the objective of this work is to investigate the flame structure and the unsteady behavior including NO_x formation in a turbulent flow field. Using the GRI [Gas Research Institute] chemical reaction mechanism (NO_x formation included)[8], a numerical analysis is carried out by solving unsteady, two-dimensional conservation equations. Fuel injection velocity is varied so that the flow becomes

* Received 30th June, 1999. Japanese original: Trans. Jpn. Soc. Mech. Eng., Vol. 65, No. 630, B(1999), p. 783-789 (Received 11th May, 1998)

** Department of Mechano-Informatics and Systems, Graduate School of Engineering, Nagoya University, Furo-cho, Chikusa-ku, Nagoya 464-8603, Japan. E-mail: yamashita@mech.nagoya-u.ac.jp

turbulent with the possibility of flame extinction downstream. Using detailed chemical kinetics, multidimensional simulations of jet diffusion flames were recently carried out for the laminar flow field[9]–[12]; only a few calculations were made for the turbulent flow field[7], including the recent DNS of a hydrogen-oxygen mixing layer[13],[14]; however, the formation of NO_x was not considered.

In connection with the present work, a study based on the laminar flamelet model was recently conducted to investigate methods of estimation of nitrogenous oxides emissions from turbulent jet diffusion flames[15], with the aim of realizing a quantitative evaluation of actual three-dimensional turbulent combustion fields. We want to extend our previous study[7] about extinction and attempt to verify the hypothesis used in this model[16], taking into account the NO_x formation process.

We treat only the two-dimensional transitional flow with a large-scale coherent fluctuation in this study. The physical effect of unsteady flow on the flame characteristics is the same as that of a three-dimensional turbulent flow with a small-scale fluctuation. We consider that the present study intermediates and fills a gap between the steady laminar flame and the turbulent flame.

2. Analytical Model and Calculation Method

2.1 Analytical model

Figure 1 shows an outline of the analytical model and boundary conditions. A Cartesian coordinate system is employed such that x is in the principal flow direction, y is in the transverse direction and the origin is at the center of the injector exit. Here, u and v are the velocity components in the x and y directions, respectively, T is the temperature and Y_i is the mass fraction of species i. We assume atmospheric pressure and room temperature $T_0=T_\infty=300$ K ($T_\infty/T_0=1$) and that the co-flowing air is composed of $Y_{O_2,\infty}=0.232$ oxygen and $Y_{N_2,\infty}=0.768$ nitrogen.

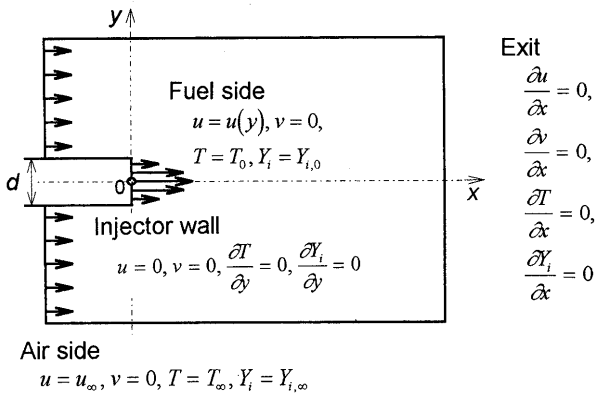

Fig. 1 Analytical model and boundary conditions

Methane is injected through an injector of width d with a fully developed velocity distribution at mean velocity u_0, uniform temperature T_0 and species mass fraction $Y_{i,0}$, into a co-flowing air stream of uniform velocity u_∞, temperature T_∞ and mass fraction $Y_{i,\infty}$. Here, the subscripts 0 and ∞ correspond to the injector exit (fuel side) and the outer flow (air side), respectively. Outer flow velocity is fixed at $u_\infty=4$ m/s, the injector diameter is 1 mm and the size of the computational domain is $x=-2.9\sim66.9$ mm, $y=-17.2\sim17.2$ mm.

Chemical reactions are described by the GRI mechanism (NO_x reactions included) in which 49 species with 279 elementary reactions are considered[8].

The governing conservation equations are the overall continuity equation, the Navier-Stokes equation, the energy equation, the species continuity equation and the equation of state[17].

$$\frac{\partial \rho}{\partial t}+\nabla\cdot(\rho \boldsymbol{v})=0$$

$$\frac{\partial(\rho u_m)}{\partial t}+\nabla\cdot(\rho \boldsymbol{v} u_m)-\nabla\cdot(\mu\nabla u_m)=-\frac{\partial P}{\partial x_m}-\rho g_m+\left(-\frac{\partial \mu}{\partial x_m}\frac{\partial u_j}{\partial x_j}+\frac{\partial \mu}{\partial x_j}\frac{\partial u_j}{\partial x_m}\right)$$

$$\frac{\partial(\rho T)}{\partial t}+\nabla\cdot(\rho \boldsymbol{v} T)-\frac{1}{c_p}\nabla\cdot(\lambda\nabla T)=\frac{1}{c_p}\frac{Dp}{Dt}-\frac{1}{c_p}\sum_i h_i w_i-\frac{\rho}{c_p}\sum_i (c_{p,i} Y_i \boldsymbol{V}_i\cdot\nabla T)$$

$$\frac{\partial(\rho Y_i)}{\partial t}+\nabla\cdot(\rho \boldsymbol{v} Y_i)-\nabla\cdot(\rho D_i\nabla Y_i)=w_i$$

$$p=\rho R^0 T\sum_i \frac{Y_i}{m_i}$$

The Soret and Dufour effects as well as the effects of pressure diffusion are neglected. In the energy equation, energy dissipation due to viscosity is neglected and by assuming a low Mach number, the term Dp/Dt is neglected. In the calculations for the laminar two-dimensional plane counterflow diffusion flame, we assume a potential flow between the two streams of fuel and air and solve the one-dimensional equations in the nozzle direction using a similarity solution.

The non-dimensional parameters are the Reynolds number $Re_0=\rho_0 u_0 d/\mu_0$ and the Schmidt number $Sc_0=\mu_0/\rho_0 D_0$ in which the injector diameter d is taken as the representative length, u_0 as the representative velocity and the representative physical properties are ρ_0, μ_0 and D_0 at the injector exit.

We assume an ideal gas mixture. Concerning the physical properties, the thermodynamic constants are taken to be temperature-dependent, and the species' specific heats at constant pressure $c_{p,i}$ are approximated by a polynomial fit of the temperature to the JANNAF data[18]. Transport properties are calculated according to the simplified transport model

proposed by Smooke[19] in which the thermal diffusivity of the mixture is approximated by the relation:

$$\frac{\lambda}{c_p}=A\left(\frac{T}{T_0}\right)^r,\ A=2.58\times10^{-4}\ \mathrm{g/(cm\cdot s)},\ r=0.7,$$

and the species' mass diffusivity is related to the transport model via the Lewis number which takes a constant specific value for each species. The mixture viscosity is calculated by assuming a constant Prandtl number for each species.

$$\rho D_i=\frac{1}{Le_i}\left(\frac{\lambda}{c_p}\right),\ \mu=Pr\left(\frac{\lambda}{c_p}\right),\ Pr=0.75$$

2.2 Numerical calculation method

The governing equations are discretized using the finite volume method; the SIMPLE method proposed by Patankar is used for the pressure field[20]. Convective terms are computed by adopting the QUICK scheme, and the implicit scheme of second-order precision is used for the time advance. The time step is 5 μs in each of which the SOR method of iteration is used with a relaxation factor of 0.07. A high-temperature source is placed at the injector rim in order to prevent the possible blow-off of the flame at the nozzle exit. The computational mesh contains 241 and 141 grid points in the x and y directions, respectively. Concerning the counterflow diffusion flame, an interval of 15 mm is taken between the two setting positions of boundary conditions for fuel and air streams; calculation is made for 201 grid points at a time step of 1 μs. Please refer to Refs. (21) to (23) for more details regarding the calculation method.

3. Results and Discussion

3.1 Structure and unsteady behavior of flame

The fuel injection velocity is found to have the same effects on the flame structure and the unsteady behavior as those found in our previous studies where the kinetics was described by the flame sheet model[2] or the skeletal reaction mechanism[7]; by increasing the fuel injection velocity, larger fluctuations are produced downstream. The instantaneous distribution of temperature shown in Fig. 2 corresponds to a jet velocity $u_0=20$ m/s($Re_0=1\,274$) and a co-flowing air velocity $u_\infty=4$ m/s. In this case, small-scale fluctuations are produced along the central axis of the jet but they do not reach the flame.

By fixing the outer flow velocity and increasing the jet velocity, large-scale unsteady fluctuations are produced beyond the transition point downstream.

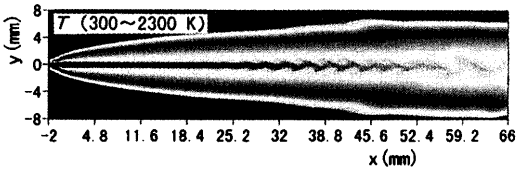

Fig. 2 Instantaneous temperature distribution ($u_0=20$ m/s, $u_\infty=4$ m/s)

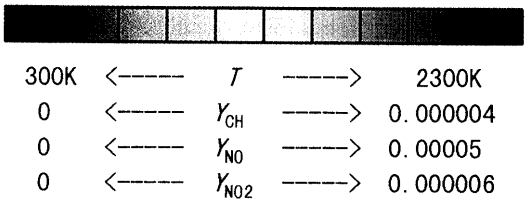

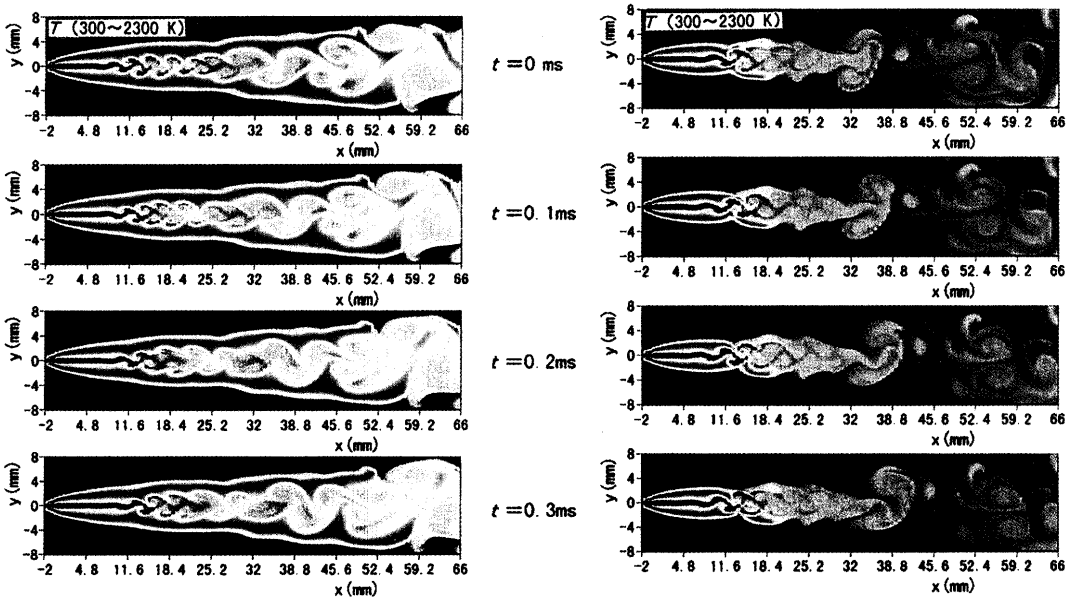

(a) $u_0=30$ m/s, $u_\infty=4$ m/s (b) $u_0=40$ m/s, $u_\infty=4$ m/s

Fig. 3 Time-dependent distributions of temperature ($t=0$, 0.1, 0.2, 0.3 ms)

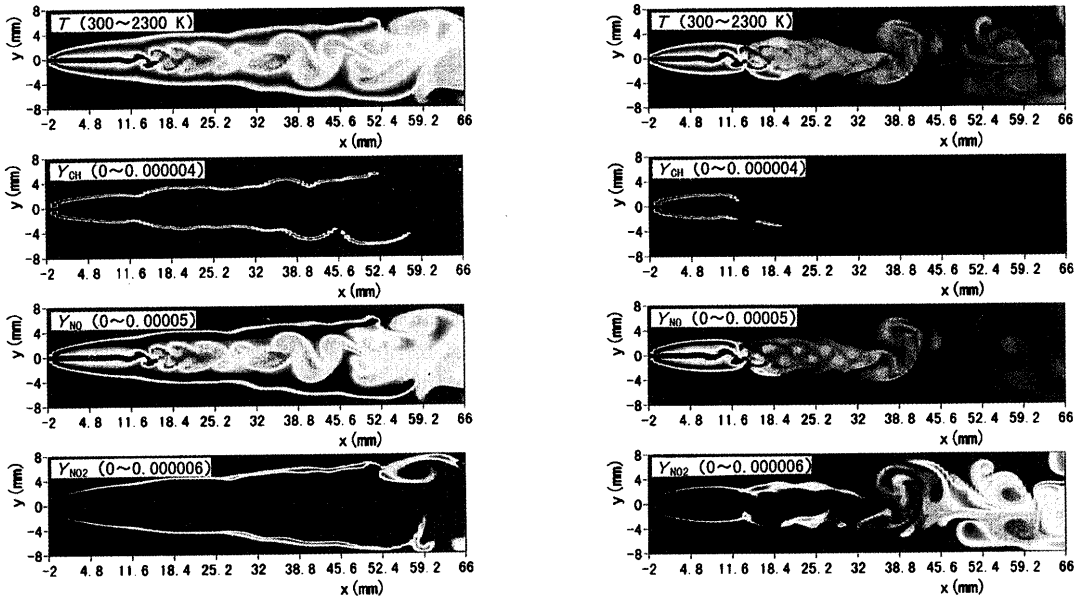

(a) u_0=30 m/s, u_∞=4 m/s (b) u_0=40 m/s, u_∞=4 m/s

Fig. 4 Instantaneous contours of T, Y_{CH}, Y_{NO} and Y_{NO_2} (t=0.3 ms)

Figures 3(a) and 3(b) show the time evolution of temperature contours, with a time interval of 0.1 ms, for two different jet velocities u_0=30 m/s (Re_0=1 911) and u_0=40 m/s (Re_0=2 548), respectively. These results are obtained after a sufficient period has elapsed for the effects of the initial conditions to be worn out completely. The instantaneous mass fraction distributions of CH, NO and NO_2 at time t=0.3 ms for the two jet velocities are shown in Figs. 4(a) and 4(b). The flame is laminar in the upstream region, having a relatively thin diffusion layer which gradually widens with the progress of diffusion downstream. It can be seen that the flame itself is now disturbed by enlarged fluctuations in the turbulent region downstream where local extinction takes place. In the figures, extinction takes place in the neighborhood of x=50 mm for the jet velocity u_0=30 m/s, while the flame is extinguished soon after the transition point for the jet velocity of u_0=40 m/s; as a result, the temperature decreases and CH radicals disappear. Moreover, NO is found to have a distribution similar to temperature; NO_2 radicals seem to peak at the outer side of the NO distribution as well as beyond the extinction point downstream where NO is converted to NO_2 by the temperature decrease.

In addition to Figs. 3 and 4, we elucidate the main characteristics of the flame in two different regions: the region of an active reaction zone (Fig. 5(a): u_0=30 m/s, u_∞=4 m/s, t=0.3 ms; x=40 mm) as well as the extinguished region of the flame (Fig. 5(b): u_0=40 m/s, u_∞=4 m/s, t=0.3 ms; x=25 mm). The two figures contain the transverse profiles of the instantaneous species mass fraction Y_i, and species mass production rate w_i along with temperature T/2 300. All variables seem to have almost symmetric distributions with respect to the central x axis and the reaction zone of both sides is seen to have the same structure. In Fig. 5(b), the flame is totally extinguished but NO_2 is found to increase due to the decrease in flame temperature during the extinction process. An expanded view of w_i distribution in Fig. 5(a) is shown in Fig. 5(c).

3.2 Comparison with the laminar counterflow diffusion flame

Studies have been carried out to investigate the validity of the laminar flamelet model (LFM) in which a hypothesis is made that "the instantaneous local structure of the turbulent flow field can be accurately simulated by the steady laminar diffusion flame"[16]. Using detailed kinetics, a comparative investigation was conducted[15] for the different laminar flow fields to which a similarity solution is applicable. The scalar dissipation rate SDR at the reaction zone was then used as a combination parameter between the turbulent and laminar flow fields and the hypothesis of this model was shown to be justified. Another study was conducted for the two-dimensional steady laminar coaxial flow field[12]. In addition, the jet flow field was investigated by Smooke et al.[10] who focused on the mixture fraction and did not make use of the SDR. The applicability of LFM was proved in our previous study[7] on the unsteady flame that included extinction, by adopting the skeletal chemical reaction scheme; in the present study, however, we want to extend our investigation to NO_x formation in unsteady turbulent jet flames.

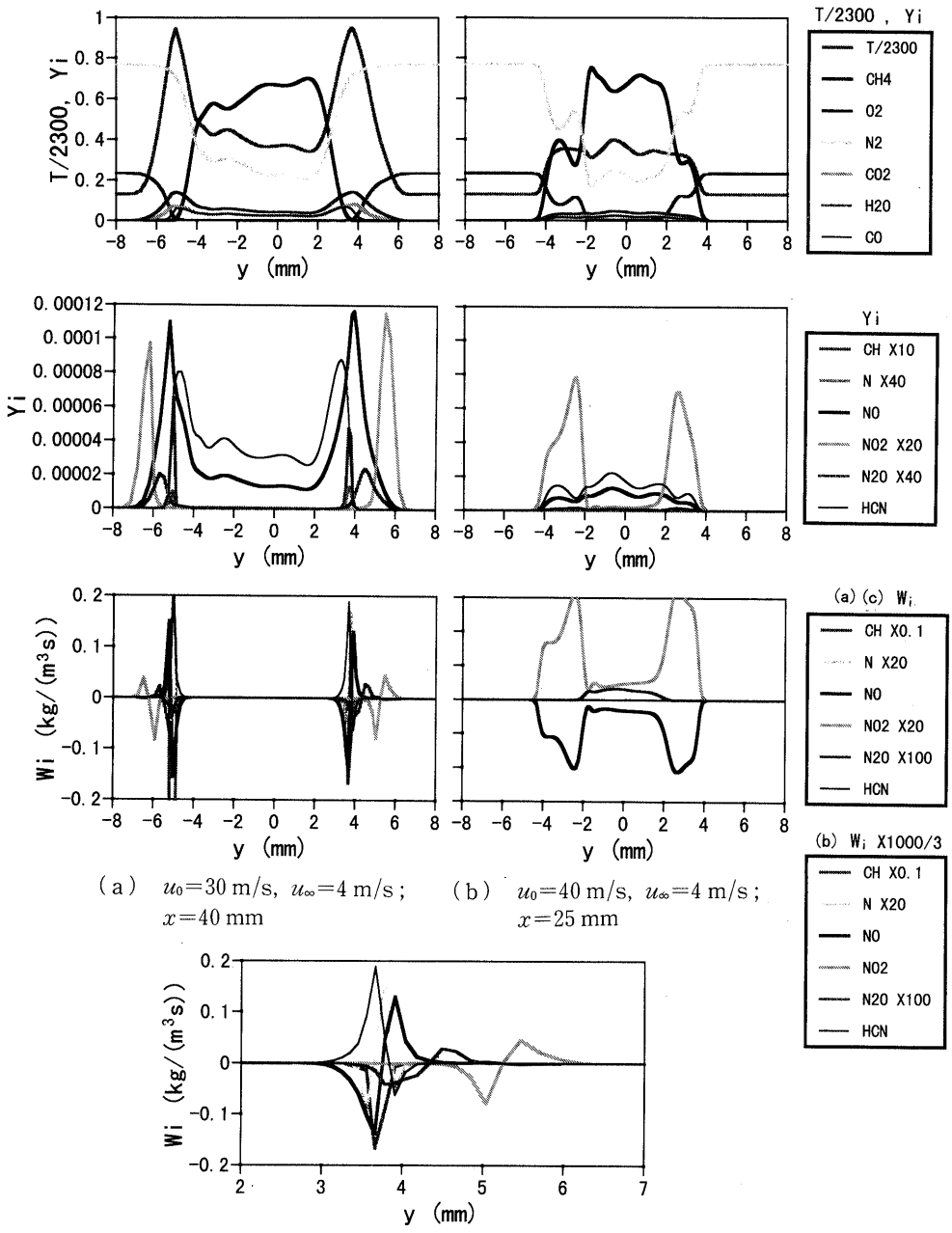

(a) u_0=30 m/s, u_∞=4 m/s; x=40 mm (b) u_0=40 m/s, u_∞=4 m/s; x=25 mm

(c) Expanded view of w_i distribution for (a)

Fig. 5 Instantaneous transverse distributions of T, Y_i and w_i (t=0.3 ms)

Figure 6(a) shows the transverse profiles of species mass fraction Y_i and species mass production rate w_i for the corresponding steady laminar two-dimensional counterflow diffusion flame (velocity gradient 13.33 s^{-1}). When the velocity gradient is comparatively large in the steady laminar flow diffusion flame, Takeno and Nishioka[24] showed that NO_x formation is dominated by the prompt NO mechanism using the C2-Chemistry of Miller and Bowman[25]. In the prompt NO mechanism, HCN is generated from N_2 in air via the elementary reaction CH + N_2= HCN+N, and HCN is converted into NCO, CN or NH immediately or indirectly and further into N. NO is chiefly generated from N via the elementary reaction N+OH=NO+H. Part of the generated NO is thus converted into HCNO, HNO and HCN in the flame.

Starting from the value shown in Fig. 6(a) as the initial value at t=0, the velocity gradient was suddenly increased by eight times, resulting in extinction[24]; the profiles corresponding to the instants t=0.6 ms and t=1.0 ms during the unsteady extinction process are shown in Figs. 6(b) and 6(c), respectively. By comparing Fig. 5(a) with Fig. 6(a) when the flame exists, or Fig. 5(b) with Fig. 6 (b) when the flame does not exist, both profiles of temperature, species concentrations and production rates (at y=1~7 mm,

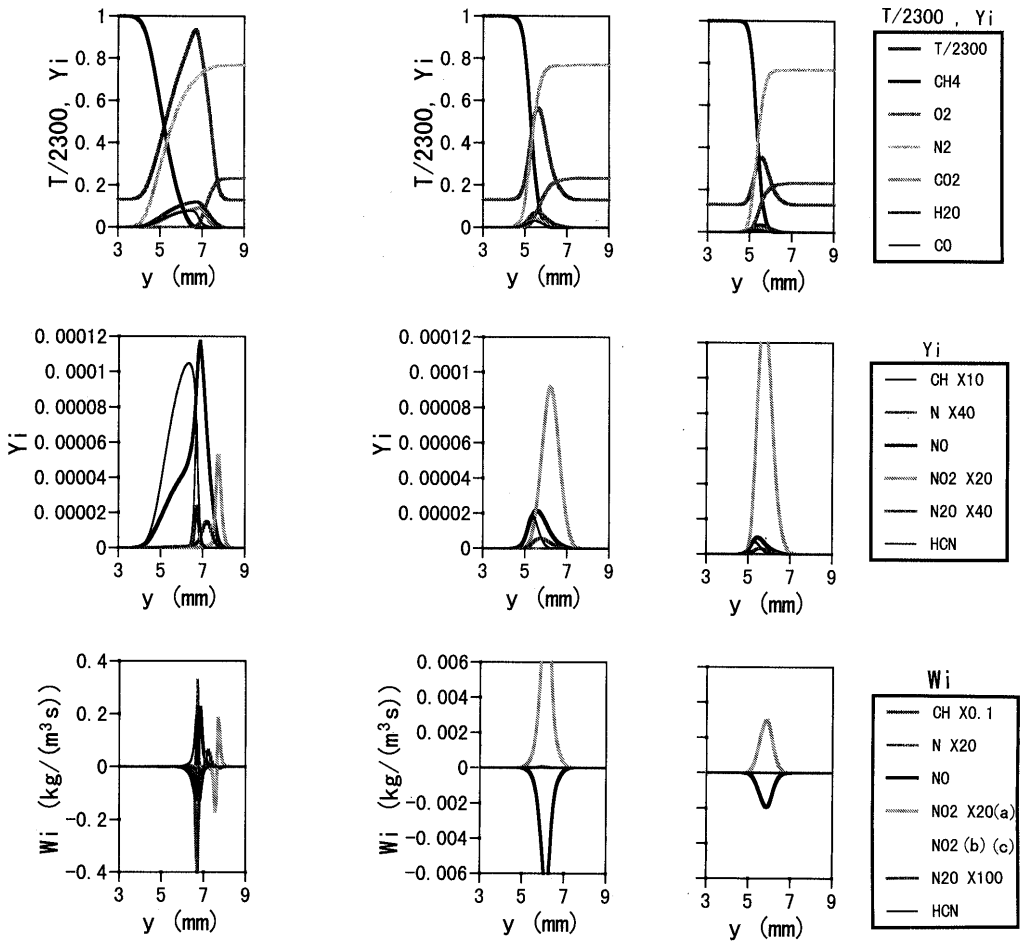

(a) Steady (t=0) (b) Unsteady (t=0.6 ms) (c) Unsteady (t=1.0 ms)

Fig. 6 Instantaneous transverse distributions of T, Y_i and w_i (Steady and unsteady counterflow laminar diffusion flame, velocity gradient 13.33～13.33×8 s^{-1})

y=−2～−8 mm in Fig. 5, and at y=3～9 mm in Fig. 6) show almost the same flame structure. Furthermore, the convective effects of the fluctuations produced in the downstream of the turbulent jet flame were found to be in good correspondence with those produced by increasing the velocity gradient in the laminar counterflow flame. In this way, it is proved that the laminar flamelet approach can be applied to the unsteady turbulent jet flame that includes extinction and takes into account the NO_x formation process. Here, the turbulent jet flame was selected to fit the laminar counterflow flame; however, it is necessary to consider an appropriate combination parameter[15] in order to realize good correspondence; this requires further investigation[26].

4. Conclusions

Based on the conservation equations of the unsteady two-dimensional flow field, a numerical analysis is carried out using the GRI chemical reaction mechanism (NO_x included) in order to elucidate the mechanism of NO_x formation in turbulent flow fields. This study has led to the following conclusions:

(1) The fuel jet velocity was found to have the same effects on the flame structure and the unsteady behavior as those concluded from the flame sheet approach; by increasing the jet velocity, the flow becomes turbulent with large fluctuations in the downstream, and the flame is disturbed by the enlarged fluctuations in the turbulent region downstream where local extinction takes place.

(2) From a comparison with the laminar counterflow diffusion flame, it was concluded that the hypothesis of the laminar flamelet model that "the instantaneous local structure of the turbulent flow field can be accurately simulated by the laminar diffusion flame", can be applied to the unsteady turbulent jet flame that includes the possibility of extinction and takes into account the NO_x formation process.

(3) As a result, it was verified that the formation of NO_x in the turbulent flow field has the same mechanism as that in the unsteady laminar diffusion

flame even for the case of extinction.

Acknowledgments

This work was partially supported by a Grant-in-Aid for Scientific Research from the Ministry of Education, Science, Sports and Culture of Japan (No. 09650234), to whom I express my gratitude. I would like to extend my sincere thanks to Ms. D. Djamrak for her kind help. The numerical calculations were performed on the supercomputer of the Computation Center of Nagoya University. I would like to express my gratitude to the staff of the Center.

References

(1) Takeno, T., Twenty-Fifth Symposium (International) on Combustion, The Combustion Institute, Pittsburgh, (1994), p. 1061-1073.
(2) Yamashita, H., Kushida, G. and Takeno, T., Proc. R. Soc. Lond., A431, (1990), p. 301-314.
(3) Yamashita, H., Kushida, G. and Takeno, T., Proc. 24th Symp. (Int.) Combust., The Combustion Institute, Pittsburgh, (1992), p. 311-316.
(4) Yamashita, H., Idota, T. and Takeno, T., Trans. Jpn. Soc. Mech. Eng., (in Japanese), Vol. 62, No. 595, B (1996), p. 1226-1233.
(5) Yamashita, H., Shimada, M. and Takeno, T., Proc. 26th Symp. (Int.) Combust., The Combustion Institute, Pittsburgh, (1996), p. 27-34.
(6) Yamashita, H., Proc. Thirty-third Japanese Symposium on Combustion, (in Japanese), (1995), p. 341-343.
(7) Yamashita, H., Djamrak, D. and Takeno, T., Role of Elementary Reactions in Flame Structure and Unsteady Behavior of Two-Dimensional Fuel Jet Diffusion Flame, JSME International Journal, Series B, Vol. 42, No. 4 (1999), p. 699-707.
(8) GRI, http: //www.me.berkeley.edu/gri_mech/, 1995.
(9) Prasad, K. and Price, E.W., Combust. Flame, Vol. 90 (1992), p. 155-173.
(10) Smooke, M.D., Xu, Y., Zurn, R.M., Lin, P., Frank, H. and Long, M.B., Proc. 24th Symp. (Int.) Combust., The Combustion Institute, Pittsburgh, (1992), p. 813-821.
(11) Katta, V.R. and Roquemore, W.M., Combust. Flame, Vol. 102 (1995), p. 21-40.
(12) Nishioka, M., Takemoto, Y., Yamashita, H. and Takeno, T., Proc. 26th Symp. (Int.) Combust., The Combustion Institute, Pittsburgh, (1996), p. 1071-1077.
(13) Tanahashi, M. and Miyauchi, T., Proc. Thirty-third Japanese Symposium on Combustion, (in Japanese), (1996), p. 59-61.
(14) Hirai, S., Okazaki, K., Touchi, H. and Kamijo, S., Proc. Thirty-third Japanese Symposium on Combustion, (in Japanese), (1996), p. 65-67.
(15) Yamashita, H., Nishioka, M. and Takeno, T., Energy Convers. Mgmt, Vol. 38, No. 10-13, (1997), p. 1343-1352.
(16) Peters, N., Prog. Energy Combust. Sci., Vol. 10 (1984), p. 319-339.
(17) Williams, F.A., Combustion Theory, 2nd ed., (1985), p. 2-3, Benjamin/Cummings.
(18) Kee, R.J., Rupley, F.M. and Miller, J.A., CHEMKIN-II: A Fortran Chemical Kinetics Package for the Analysis of Gas-Phase Chemical Kinetics, SAND89-8009, (1989).
(19) Smooke, M.D., Reduced Kinetic Mechanisms and Asymptotic Approximations for Methane-Air Flames, (1991), p. 1-28, Springer-Ver lag.
(20) Patankar, S.V., Numerical Heat Transfer and Fluid Flow, (1980), p. 126-130, McGraw-Hill.
(21) Yamashita, H., Simulation of Heat and Flow, (in Japanese), (1995), p. 205-240, Maruzen.
(22) Yamashita, H., Program of Numerical Simulation for Turbulent Flame, Computation Center News, (in Japanese), Vol. 26, No. 3 (1995), p. 194-215, Nagoya Univ.
(23) Yamashita, H., User's Manual for Program of Numerical Simulation for Turbulent Flame Using Detailed Chemical Kinetics, (in Japanese), (1997), p. 1, Computation Center of Nagoya University.
(24) Takeno, T. and Nishioka, M., Nensyo Kenkyu, Vol. 111 (1998), p. 3-15.
(25) Miller, J.A. and Bowman, C.T., Prog. Ener. Combust. Sci., Vol. 15 (1989), p. 287-338.
(26) Muramatsu, A., Yamashita, H. and Takeno, T., Proc. Thirty-fifth Japanese Symposium on Combustion, (in Japanese), (1997), p. 317-319.